

Research Article

The Possible Therapeutic Role of Probiotic on Cyclophosphamide Damaging Effects in Adult Male Albino Rat Jejunum



Rasha Mohamed Tantawi¹, Sara Mohamed Naguib¹,
Nashwa Fathy Eltahawy¹ and Soha Abdel-kawy Abdel-Wahab¹

¹Department of Histology and Cell Biology, Faculty of Medicine, Minia University,

DOI: 10.21608/mjmr.2023.196128.1357

Abstract

Background: Cyclophosphamide (CP) is extensively used as an antineoplastic drug but unfortunately, it is cytotoxic, to the intestinal mucosa. Probiotics have beneficial effects on the intestinal mucosa. **Aim of the work:** The current study aimed to investigate the possible protective effects of probiotics against the structural and biochemical changes that occur in the rat jejunum after CP administration, and to address some of the underlying mechanisms of these effects. **Materials and methods:** Thirty-six adult male albino rats were randomly divided into six groups: the C-group, Prob-group, CP-2D group, CP-2w group, Prob-CP-2D group, Prob-CP 2W group. Blood samples were collected for serum IL-10 level assay. Jejunum specimens were excised for histological, immune-histochemical, and morphometric studies. Other tissue specimens were proceeded for estimation of MDA and GSH levels. **Results:** The results showed marked morphological and biochemical changes in CP-2D group that decreased in CP-2W and Prob-CP-2D groups but still with a significant difference if compared to the control group. Moreover, the Prob-CP-2W group displayed a marked improvement of all previously mentioned data. **Conclusion:** It can be concluded that the administration of probiotics ameliorated the toxic effect of CP on jejunum through their anti-inflammatory, anti-oxidative, and anti-apoptotic effects.

Keywords: Probiotic, Cyclophosphamide, Rat, jejunum

Introduction

Cyclophosphamide (CP) is considered as one of the most successful chemotherapeutic drugs which are listed on the World Health Organization List of Essential Medicines. It has been widely used to treat a range of cancers since its initial synthesis in 1958 (Madondo et al., 2016). It remains a mainstay in the treatment of hematological malignancies such as lymphoma, leukemia, and various epithelial tumors including breast, ovarian and small-cell lung cancers (Ahlmann and Hempel, 2016). High dose of CP is currently used as an immunosuppressant for the treatment of autoimmune diseases such as lupus. It is also used in bone marrow transplantation because it causes lymph depletion (Madondo et al., 2016).

In spite of its beneficial effects, it has many side effects (Farkas et al., 2019) even when given at low doses which include petechial hemorrhage in the small bowel, abdominal pain, diarrhea, and inflammation (Alhowail et al., 2019). The CP caused severe tissue oxidative stress and massive cellular damage, consequently increasing apoptosis and death of both cancer and healthy cells (Abdel-Hafez et al., 2017b). It affects the mucosal barrier and changes the microbial composition in the small intestine (Shi et al., 2017). It can injure self-renewing immune cells and intestinal epithelial cells, resulting in enteritis by enhancing intestinal permeability and impairing the host immune system. The side effects caused by CP

are one of the main obstacles to successful cancer treatment (Wang et al., 2019).

Probiotic bacteria have beneficial effects on the intestinal epithelium (Satish Kumar et al., 2015). Greater clinical interest for probiotics has focused on either preventing or treating gastrointestinal infections and diseases. Previous research had suggested their use as a treatment approach for intestinal mucositis (Gerhard et al., 2017). It was documented that probiotics could prevent gut inflammatory processes *via* regulating the intestinal barrier permeability and production of antimicrobials (de LeBlanc and LeBlanc, 2014). Moreover, they have various mechanisms such as modulation of the mucosal immune system, alteration of the intestinal microflora, enhancing the degradation of enteral antigens (Kumar et al., 2015), and a suppressive effect on the oxidative stress by inhibiting lipid peroxidation (Wu et al., 2019a).

Probiotics also have an antiapoptotic effect as they enhance epithelial cell proliferation of both small and large intestine by increasing short chain fatty acids (SCFA) production (Li et al., 2015a). It was reported that SCFAs are important for maintaining intestinal epithelial integrity by stimulating epithelial cell proliferation and mucus secretion and promoting tissue repair and wound healing (Thorburn et al., 2014).

This study aimed to investigate the possible therapeutic effects of probiotics against structural and biochemical changes that occur in the jejunum of adult male albino rats after CP administration. We also try to clarify some of the underlying mechanisms of these beneficial effects.

Materials and Methods

In the present study, thirty-six adult (8-12 weeks) male albino rats were used, each weighing between 150-250 g. The study was performed in accordance to the guidelines approved by the Minia University institutional Ethics Committee for use of laboratory animals (Approval NO. 315).

Reagents:

1- Probiotic (Lacteolfort®) sachets (each sachet contains 10 billion Lactobacillus,

corresponding to Lactobacillus delbruekii and Lactobacillus fermentum) were purchased from Rameda company, Egypt. Each sachet was dissolved in 20 ml distilled water before administration to rats at a dose of 10 billion lactobacillus /rat /day divided into two doses by oral gavage twice daily (Kumar et al., 2015).

2- Cyclophosphamide (Endoxan®) vial containing 1gm of cyclophosphamide was purchased from Multipharma company, Egypt. It was diluted in 50 cm physiological saline and used as a single sublethal dose of 300 mg/ kg body weight via 3 cm intraperitoneal injection at the beginning of the experiment (Owari et al., 2012).

Experimental design

Thirty-six rats were randomly divided into the following six groups (6 rats each):

1. The control group (C-group): rats received standard rat diet and water for two weeks.
2. The probiotic group (Prob-group): rats received probiotics as previously mentioned.
3. The cyclophosphamide 2 days group (CP-2D): rats received the single mentioned dose of CP and were sacrificed after 2 days of injection
4. The cyclophosphamide 2 weeks group (CP-2W): rats received the single injection of CP then sacrificed after 2 weeks of injection.
5. The probiotic-cyclophosphamide 2 days group (Prob-CP-2D): rats received CP followed by 2 days of probiotics as the previously mentioned then were sacrificed after the 2 days of probiotics intake.
6. The probiotic- cyclophosphamide 2 weeks group (Prob-CP-2W): rats received CP followed by 2 weeks of probiotics and were sacrificed after the 2 weeks of probiotics intake.

Rats were sacrificed by decapitation under light halothane anesthesia. Specimens of the jejunum (5 cm distal to the duodenum) were rapidly removed and carefully dissected for tissue preparation. After rinsing in normal saline, parts of jejunum specimens were rapidly fixed in 10% formal saline for 48 hours, then washed by tap water and processed to prepare paraffin sections for the histological, immunological, and morphometric study. Other parts were used for tissue homogenates preparation for the biochemical study.

Histological studies

Light microscopic study

For light microscopic examination, jejunal specimens were fixed in 10% formal saline and processed to obtain the paraffin blocks. Serial (5- μ m) sections were stained with hematoxylin and eosin (H&E) and PAS stain (Suvarna et al., 2018). Additionally, immunohistochemical staining was performed by using monoclonal rabbit antibody for Ki-67 (proliferative marker) (Catalogue number. SAB5500134, Sigma Aldrich, Egypt) and polyclonal rabbit antibody for cleaved caspase-3 (apoptotic marker) (Catalogue number. PA1-26426, Thermo Fisher, USA). Immunohistochemistry

for both antibodies was performed on formalin-fixed, paraffin-embedded tissue. The procedure was done according to the manufacturer's instructions. The positive control for anti-Ki-67 was taken from normal rat hair follicle while the positive control for caspase-3 antibody was taken from human tonsillar tissue.

This substrate gives brown color at the immunoreactive sites. Regarding the anti-activated caspase 3, expression was mainly at the cytoplasm of immune positive cells, but it may be nuclear and/or cytoplasmic. While the expression of anti-Ki-67 antibody was nuclear.

Biochemical study

Laboratory analysis was done at the Pharmacology Department, Faculty of Medicine, Minia University.

Measurement of tissue malondahyde (MDA) and glutathione (GSH)

Jejunal tissues were homogenized in 1:10 (weight: volume) phosphate buffer (pH 7.4) using a Teflon headed homogenizer at a speed of 2500 rpm. Triton x100 and protease inhibitor cocktail were added. The homogenates were centrifuged at 6.000g for 10 minutes at 4°C. The resulting supernatant was used for colorimetric determination of jejunal MDA (Uchiyama and Mihara, 1978) and GSH (Moron et al., 1979) using commercially available kits (Bio diagnostic, Egypt) using the spectrophotometer (Jenway 7305, Staffordshire, UK).

Measurement of plasma level of interleukin-10 (IL-10):

A serum separator tube was used, and samples were allowed to clot for two hours at room temperature or overnight at 4° C before centrifugation for 15 min at 1000 xg. The resulting serum was stored at -80°C for analysis within 1 week. The plasma level of interleukin-10 (IL-10) was measured by a quantitative enzyme-linked immunosorbent assay (ELISA) kit (Catalogue number CSB-E04595r, Cusabio, China) according to the manufacturer instructions (Hassan et al., 2019).

Image capture and morphometric study

In Histology and Cell Biology Department, Faculty of Medicine, Minia University, an Olympus light microscopy (Olympus BX 40, Japan) was used for examining and capturing images for the histological and immunohistochemical sections. Slides were photographed using an Olympus digital camera (Olympus, Japan). Images were saved as jpg. The morphometric study was done using Leica QWin 500 image analysis software (Leica Microsystems, Wetzlar, Germany) from 10 non-overlapping fields from each rat of the studied groups.

Measuring the mean number of jejunal villi, mean height, and width of the jejunal villi, and the mean depth of crypts.

The mean number of villi (using power X10), the mean height and width of the villi, and the depth of crypts (using power X100) in H&E-stained sections were measured in micrometers. The villus height was measured from the crypt-villus junction to the tip, while crypt depth was measured from the crypt-villus junction to the base. The width of the intestinal villi was also analyzed (Shang et al., 2020).

Counting of goblet cells and Ki-67 immune positive cells.

The mean number of goblet cells (using power X100) from PAS stained sections (Ying et al., 2020) and the mean number of Ki-67 immune positive cells from their immune-stained sections (using power X400) were counted.

Measuring the mean area fraction of activated caspase-3 immune reactivity

The mean area fraction of activated caspase-3 was measured in a standard measuring frame per 10 photomicrographs from each rat (using X 100).

Statistical analysis

Numerical data were obtained firstly from the used software to Microsoft Excel and were then transferred to Graph Pad Prism (version 5.01 for Windows, Graph Pad Software, San Diego, California, USA, www.graphpad.com) for analysis. Data were represented as mean \pm standard deviation (Mean \pm SD). The significant differences among each 2 groups were done via the student t-test and the one-way ANOVA followed by the Tukey-Kramer post hoc test for multiple comparisons. P-values of <0.05 considered statistically significant.

Results

The histological results

Hematoxylin and Eosin results

Microscopic examination of the jejunal control and probiotic sections showed normal typical architecture of the small intestine. It was consisted of four layers; mucosa, submucosa, musculosa and serosa. The mucosa showed both villi and crypts. The villi appeared long-leaf like projections and covered by simple columnar absorptive epithelium (enterocytes) with goblet cells. Enterocytes: the predominant epithelial cell type, had eosinophilic cytoplasm and basal pale oval nuclei. Its apical surface was covered by a regular continuous brush border. Among the numerous absorptive cells, interspersed goblet cells were scattered in crypts and villi which decreased towards the villus tip. The apical end of each goblet cell was occupied by a large mass of mucus displacing its intensely stained nucleus basally. The core of the villi named the lamina propria and the submucosa were formed of loose connective tissue. Crypts were lined by different cell types and the Paneth cells lined the base of these crypts and were characterized by their apical eosinophilic granules. The muscle fibers were orderly arranged, and the serosal connective tissue was covered by the mesothelial lining (Fig. 1a-b, 2 a-b, 3 a-b). Regarding the CP-2D group, it showed preservation of the four layers of the jejunum but with marked various patchy morphological

changes. The mucosa showed loss of most of its villi. The remnant infrequent villi showed distortion, appeared shorter and broader. Most epithelial cells lining of the mucosa were shredded and frequently seen in the lumen leaving bare areas of mucosa. Lamina propria showed congested blood capillaries as well as inflammatory cell infiltration. Crypts appeared deeper and longer. The cells lining the crypts showed signs of degeneration in the form of vacuolation, ballooning, and nuclear pyknosis. There was an absence of the characteristic acidophilic granules of Paneth cells lining the crypts. Vascular congestion was observed in the submucosa. The muscle fibers were widely separated. (Fig. 1c, 2d-c, 3c-d). The CP-2W and Prob-CP-2D groups showed more frequent villi but they showed shortening and broadening with slight shedding of the epithelial lining and appearance of sub-epithelial spaces, edema. In addition, areas of stratification of polyhedral cells with rounded nuclei were noticed. Lamina propria and submucosa showed less congested blood capillaries and less inflammatory cell infiltration if compared to the CP-2D group. The reappearance of some acidophilic granules in few Paneth cells was noticed. Musculosa still showing focal areas of widely separated muscle fibers (Fig. 1d-e, 2e-f, 3e-f).

Furthermore, Prob-CP-2W group showed more or less normal leaf-like intestinal villi with apparent covered simple columnar epithelium with goblet cells and more or less normal crypts. Normal appearance of enterocytes with oval pale basal nuclei and eosinophilic cytoplasm were noticed. Goblet cells with basal dark nuclei and broad apex filled with mucus was also observed. Absence of congestion and inflammatory cell infiltration or edema were a clear finding. Most of the Paneth cells appeared with their characteristic acidophilic granules. The muscle fibers were orderly arranged and the serosa was apparent normal (Fig. 1f, 2g, 3g).

Effect of probiotic on the morphometric changes:

There was insignificant difference in the 4 studied parameters between the C-group and the Prob-group (all $p \geq 0.05$). The CP-2D group showed a significant decrease in the number and height of the villi with a significant

increase in the width of the villi and the depth of the crypts if compared to both control and the Prob-groups (all $p < 0.05$). The CP-2W group showed a significant decrease in the number and height of the villi if compared to both control and the Prob-groups and a significant increase if compared to CP-2D group (all $p < 0.05$). Moreover, it showed a significant increase in the width of the villi and the depth of the crypts if compared to both control and the Prob-groups (all $p < 0.05$). Comparing to CP-2D group, it showed insignificant increase in the width of villi and the depth of the crypts ($p \geq 0.05$). The Prob-CP-2D group showed a significant increase in the number and height of the villi if compared to CP-2D group (all $p < 0.05$) and insignificant difference if compared to CP-2W group ($p \geq 0.05$). Moreover, its width of villi had insignificant difference if compared to CP-2D group and CP-2W group ($p \geq 0.05$), while the depth of the crypts had a significant decrease compared to CP-2D group ($p=0.007$) and insignificant difference compared to CP-2W group ($p=0.569$). The Prob-CP-2W group showed a significant increase in the number and height of villi if compared to CP-2D, CP-2W and Prob-CP-2D groups (all $p < 0.05$) with insignificant difference in the number of villi if compared to C-group ($p=0.096$). It showed a significant decrease in the width of villi and depth of the crypts if compared to CP-2D, CP-2W and Prob-CP-2D groups (all $p < 0.05$) with insignificant difference if compared to C-group and Prob-group (all $p \geq 0.05$) (Fig 4).

PAS results

The jejunal tissues from both control and probiotic groups showed a positive PAS reaction in the intact apical brush borders and basement membranes of the lining epithelium of the villi and crypts. Also, mucus in goblet cells showed positive PAS reaction. The jejunum of the CP-2D group showed loss of most of the apical brush borders and basement membranes of the lining epithelium of the damaged villi and crypts. CP-2W and Prob-CP-2D groups showed areas of focal loss of the PAS-stained brush borders and basement membranes of the lining epithelium. The Prob-CP-2W group showed preserved PAS positive reaction of most brush borders and basement membranes of the lining epithelium of the villi and crypts.. Morphometrically regarding the

number of goblet cells, there was insignificant difference in Prob-group if compared to the C-group ($p = 0.089$). The CP-2D and CP-2W groups showed a significant decrease if compared to both C-group and Prob-group (all $p < 0.05$). Meanwhile, the CP-2W group had a significant increase if compared to the CP-2D group ($p < 0.0001$). The Prob-CP-2D group showed a significant increase if compared to CP-2D group ($p < 0.0001$) with insignificant difference if compared to CP-2W group ($p = 0.065$). after 2 weeks of probiotic administration; the Prob-CP-2W group showed a significant increase if compared to CP-2D, CP-2W and Prob-CP-2D groups (all $p < 0.05$) without significant difference if compared to the C-group and Prob-group (all $p \geq 0.05$) (Fig. 5).

Immunohistochemical results:

Immunohistochemical results for Ki-67:

The control and probiotic groups showed numerous Ki-67 immune positive nuclei in epithelial lining of the jejunal crypts without a significant difference ($p = 0.364$). The CP-2D and CP-2W groups had a significant decrease in immune positive nuclei if compared with the control and Prob-groups (all $p < 0.05$) and a significant increase if compared to CP-2D group ($p = 0.0002$). The Prob-CP-2D group showed a significant increase in positive cells if compared to CP-2D group ($p < 0.0001$) and insignificant difference if compared to CP-2W group ($p = 0.203$). The Prob-CP-2W group showed a significant increase if compared to CP-2D, CP-2W and Prob-CP-2D groups (all $p < 0.0001$) with insignificant difference if compared to C-group and Prob-group (all $p < 0.05$) (Fig. 6).

Immunohistochemical results for activated caspase 3:

The Control and probiotic sections showed faint cytoplasmic and or nuclear immune reactivity for activated caspase-3 in some epithelial cells of the lining of villi of jejunal mucosa without a significant difference in the area fraction of activated caspase-3 expression ($p = 0.374$). The CP-2D group showed a significant increase if compared to both C-group and Prob-group (all $p < 0.0001$). The CP-2W group had a significant increase if compared to both C-group and Prob-group (all $p < 0.0001$) with a significant decrease compared to CP-2D

group ($p < 0.0001$). The Prob-CP-2D group showed a significant decrease compared to CP-2D group ($p < 0.0001$) and insignificant difference compared to CP-2W group ($p = 0.637$). The Prob-CP-2W showed a significant decrease compared to CP-2D, CP-2W and Prob-CP-2D groups (all $p < 0.0001$) with insignificant difference compared to C-group ($P = 0.052$) and prob-group ($p = 0.245$) (Fig.7).

Biochemical results:

There was insignificant difference in the serum level of IL-10, jejunal MDA, and GSH levels in Prob-group if compared to the C-group. The CP-2D group showed a significant decrease in the serum IL-10 and GSH levels with a

significant increase in MDA level if compared to both control and probiotic groups.

The CP-2W and Prob-CP-2D groups showed a significant increase in the serum IL-10 and jejunal GSH levels with a significant decrease in MDA level if compared to the CP-2D group and insignificant difference if compared to each other but still with a significant difference if compared to the C-group.

The Prob-CP-2W showed a significant increase in the serum IL-10 and jejunal GSH levels and a significant decrease in MDA level if compared to CP-2D, CP-2W and Prob-CP-2D groups which become nearly similar to those of C-group. (Fig.8 a, b, c).

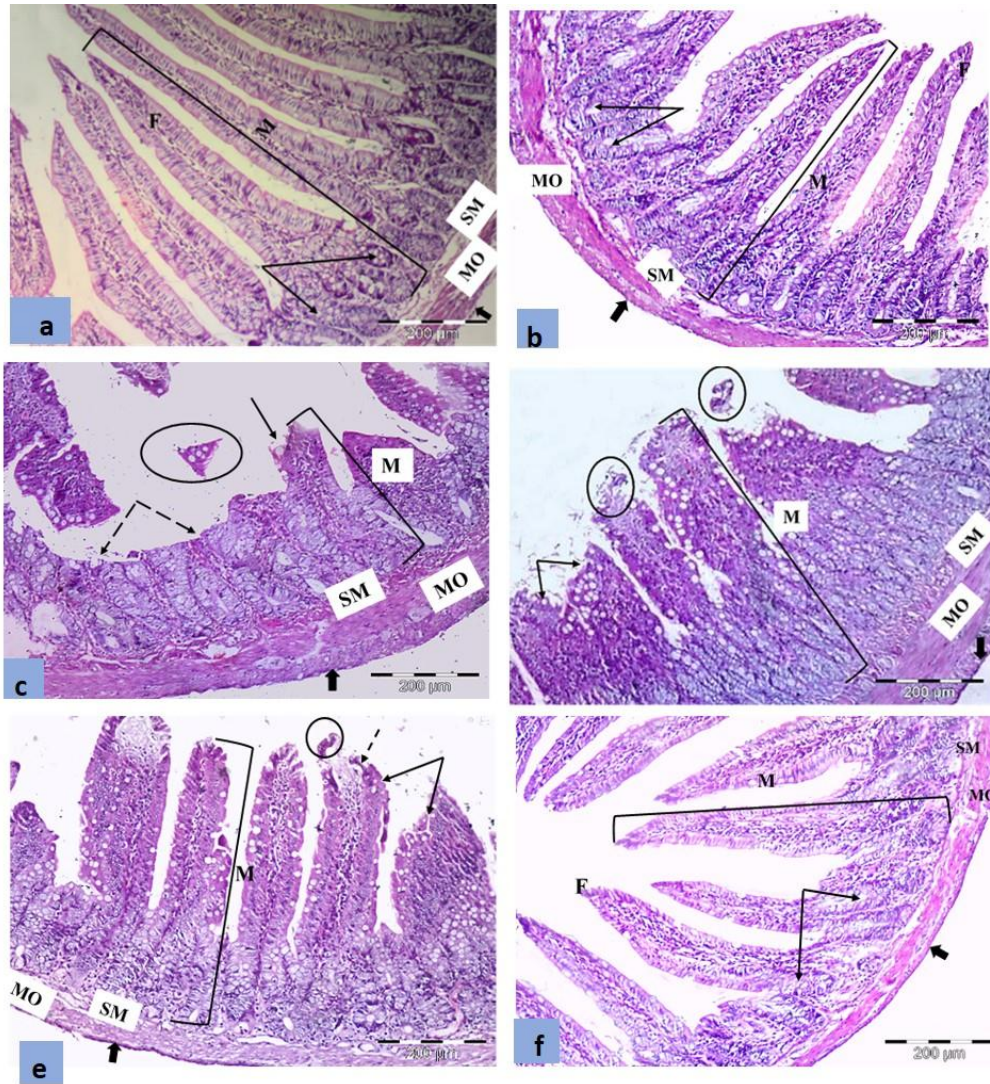


Figure (1): Representative photomicrographs of jejunum in (a) control group and (b) probiotic groups: showing normal architecture; intestinal mucosa (M), submucosa (SM), muscularis (MO), and serosa (thick arrow). Notice the leaf like villi (F) covered with simple columnar epithelium with goblet cells and the jejunal crypts (arrows). (c) CP-2D group showing distorted villi (arrow) and shredded epithelial cells in the lumen (circle) with bared mucosal areas (dashed arrows). (d) CP-2W and (e) Prob-CP-2D groups showing short, broad villi (arrows) and shedding of the villus epithelium in the lumen (circles). (f) Prob-CP-2W group showing more or less normal leaf-like intestinal villi (F) and normal crypts (arrows). H & E X 400

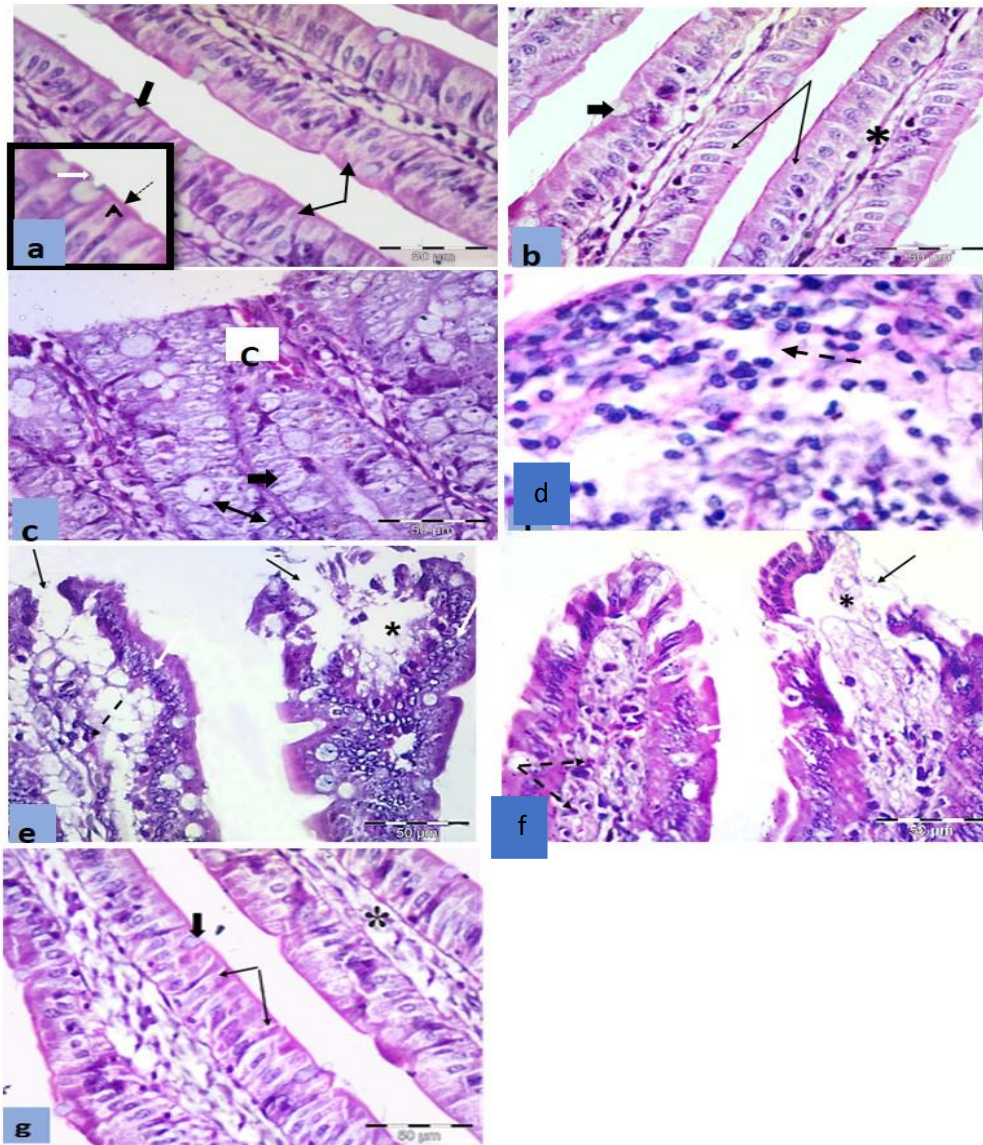


Figure (2): Representative photomicrographs of the jejunum in (a) control and (b) probiotic groups showing the villi covered by enterocytes (arrows) and goblet cells (thick arrow) with a core of connective tissue (*). Notice enterocytes with oval pale basal nuclei and eosinophilic cytoplasm. Goblet cells with basal dark nuclei and broad apex filled with mucus. The inset is a higher magnification showing the regular striated brush border (dashed arrow), the terminal web (arrowhead) and the terminal bar (white arrow). (c) CP-2D group showing congested blood capillaries in the lamina propria (c). The cells lining the crypts showing ballooning and vacuolation (thick arrow) with pyknotic nuclei (double head arrow) and absence of the characteristic acidophilic granules of Paneth cells lining the crypts. (d) CP-2D group showing inflammatory cells (dashed arrow). (e) CP-2W and (f) Prob-CP-2D groups showing damaged villous lining with bared areas (arrows) with fewer inflammatory cell infiltration (dashed arrow). Notice the subepithelial space (*) and areas of stratification of polyhedral cells with rounded nuclei (white arrows). (g) Prob-CP-2W group showing more or less normal leaf like villi covered by enterocytes (arrows) and goblet cells (thick arrow) with a core of connective tissue (*). Notice normal appearance of enterocytes with oval pale basal nuclei and eosinophilic cytoplasm and goblet cells with basal dark nuclei and broad apex filled with mucus. H & E X 400; inset X1000

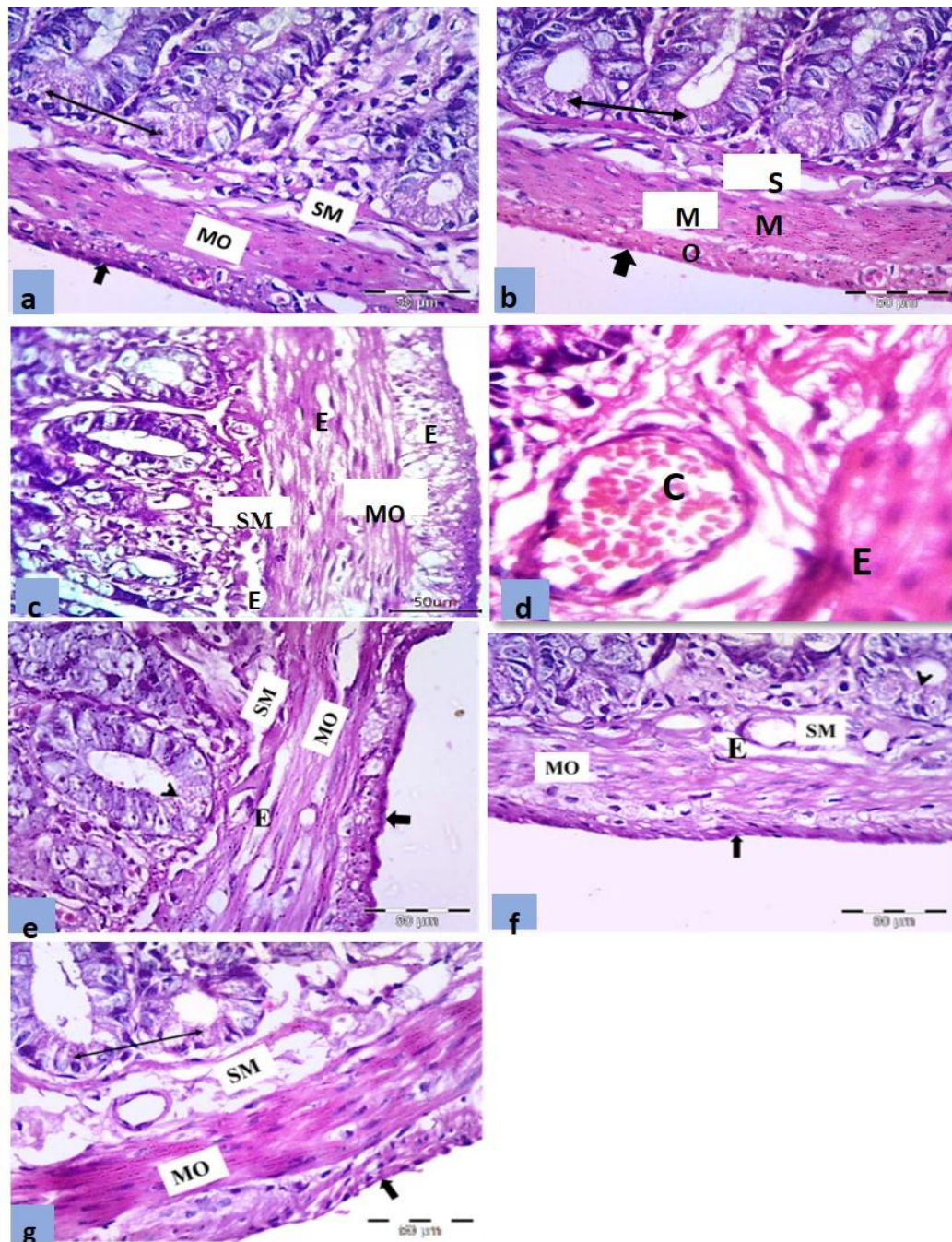


Figure (3): Representative photomicrographs of the jejunum in (a) control and (b) probiotic groups showing the apparent normal crypts in the lamina propria, the submucosa (SM), musculosa (MO) and serosa (thick arrow). Notice Paneth cells (double head arrows) deep in the crypts with their large apical eosinophilic granules. (c) CP-2D group showing edema (E) in submucosa (SM) and in muscle layers (MO). (d) CP-2D group showing congestion (c) in submucosa. (e) CP-2W and (f) Prob-CP-2D group showing reappearance of some acidophilic granules in few Paneth cells (arrowhead) while musculosa showing areas of edema (E). (g) Prob-CP-2W group showing absence of congestion, inflammatory cell infiltration or edema, and most Paneth cells with their characteristic acidophilic granules (double head arrow) The muscle fibers were orderly arranged, and the serosa was apparent normal. H & E X 400

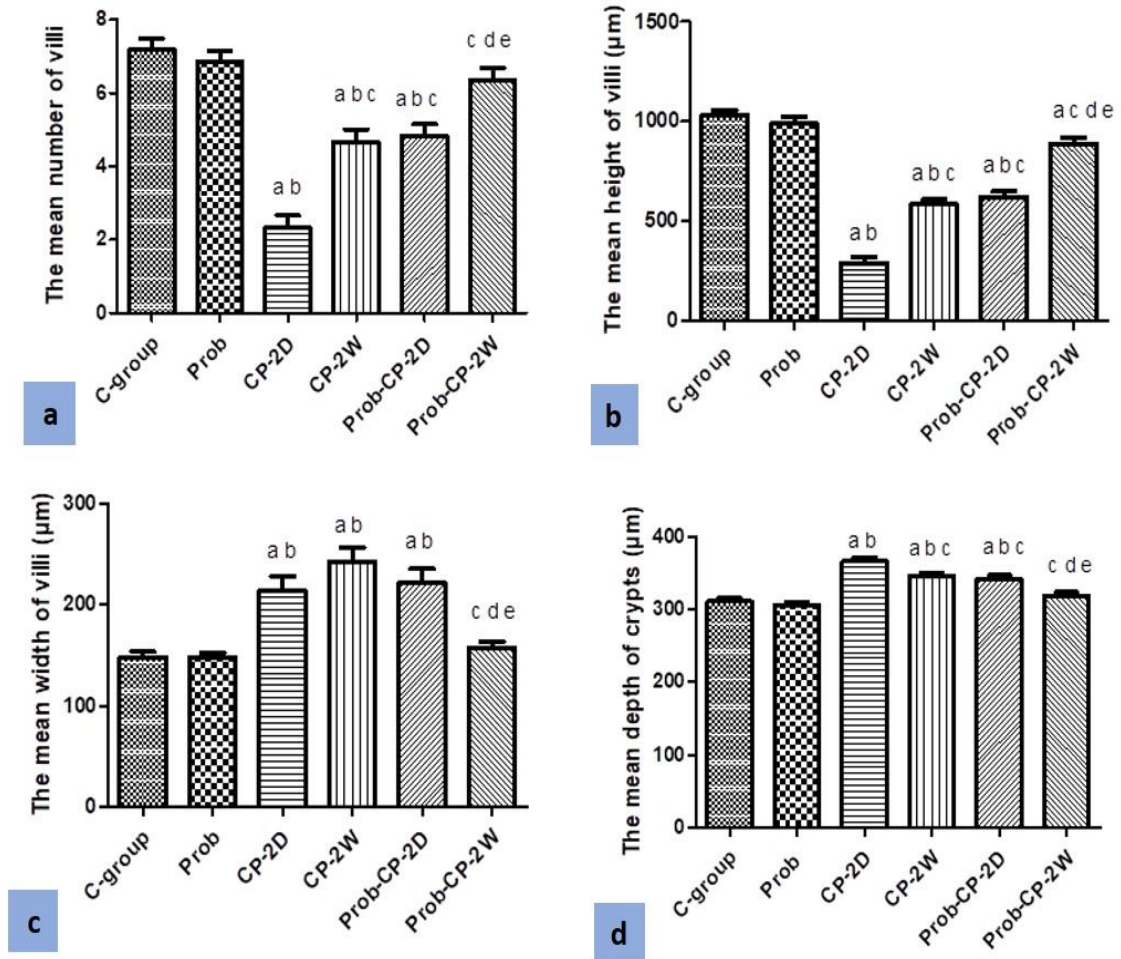


Figure (4): (a) the mean number of villi of jejunum in the studied groups (n=6), (b) the mean height of the villi (µm) (c) the mean width of the villi (µm) (d) the mean depth of the crypts (µm) in the jejunum in the studied groups (n=6). a: significant vs C-group, b: significant vs Prob-group, c: significant vs CP-2D, d: significant vs CP-2W, e: significant vs Prob-CP-2D

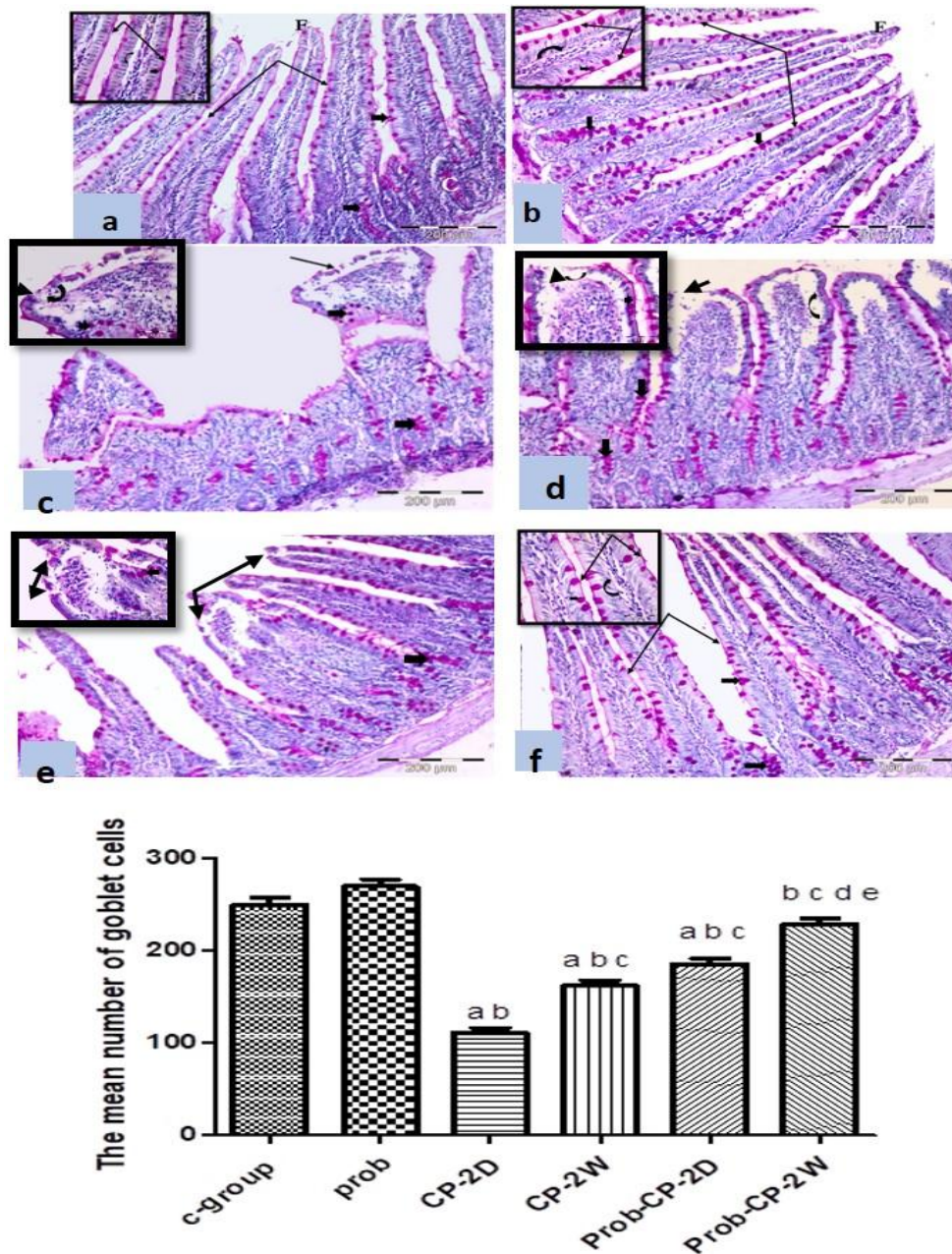


Figure (5): The representative photomicrographs of the jejunum in (a) control and (b) probiotic groups showing the intact PAS stained brush borders (arrows) and basement membranes (curved arrow) of the enterocytes and the PAS stained mucus in the scattered goblet cells (thick arrows) in the villi (F) and crypt lining. (c) CP-2D group showing loss of most apical PAS positive brush borders (arrows) and basement membranes (curved arrow) of enterocytes in damaged villi. Notice the marked decrease in goblet cells (thick arrows) within a disturbed lining. (d) CP-2W and (e) Prob-CP-2D groups showing decreased areas of focal loss of the PAS stained brush borders (arrows) and basement membranes of the enterocytes (curved arrows) with apparent increase in the number of goblet cells (thick arrows). (f) Prob-CP-2W group showing preserved PAS positive reaction of most brush borders (arrows) and basement membranes (curved arrow) of the columnar cells of the villi and apparent more increase in the number of the goblet cells (thick arrows). PAS X400. (g): The mean number of goblet cells in the jejunum in the studied groups (n=6)

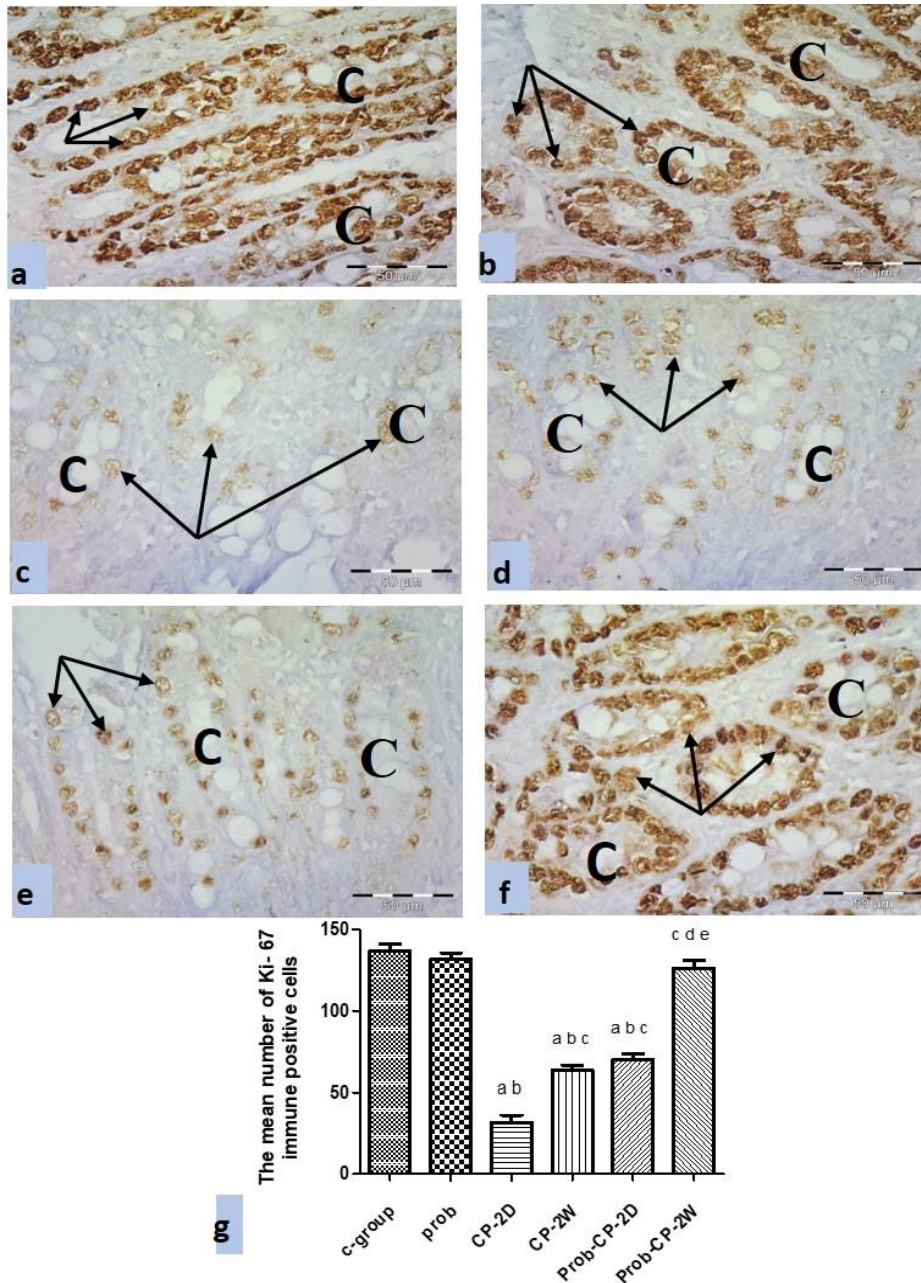


Figure (6): The representative photomicrographs of the jejunum in (a) control and (b) probiotic groups showing numerous Ki-67 immune positive nuclei (arrows) in epithelial cells lining the crypts (C). (c) CP-2D group showing marked decrease in Ki-67 immune positive nuclei (arrows) in epithelial cells lining the crypts (C). (d) CP-2W and (e) Prob-CP-2D groups showing a relative increase of Ki-67 immune positive nuclei (arrows) in epithelial cells lining the crypts (C). (f) Prob-CP-2W group showing numerous Ki-67 immune positive nuclei (arrows) in epithelial cells lining the crypts (C). Ki-67 X400. (g) The mean number of Ki-67 positive cells in the studied groups (n=6) a: significant vs C-group, b: significant vs Prob-group, c: significant vs CP-2D, d: significant vs CP-2W, e: significant vs Prob-CP-2D .

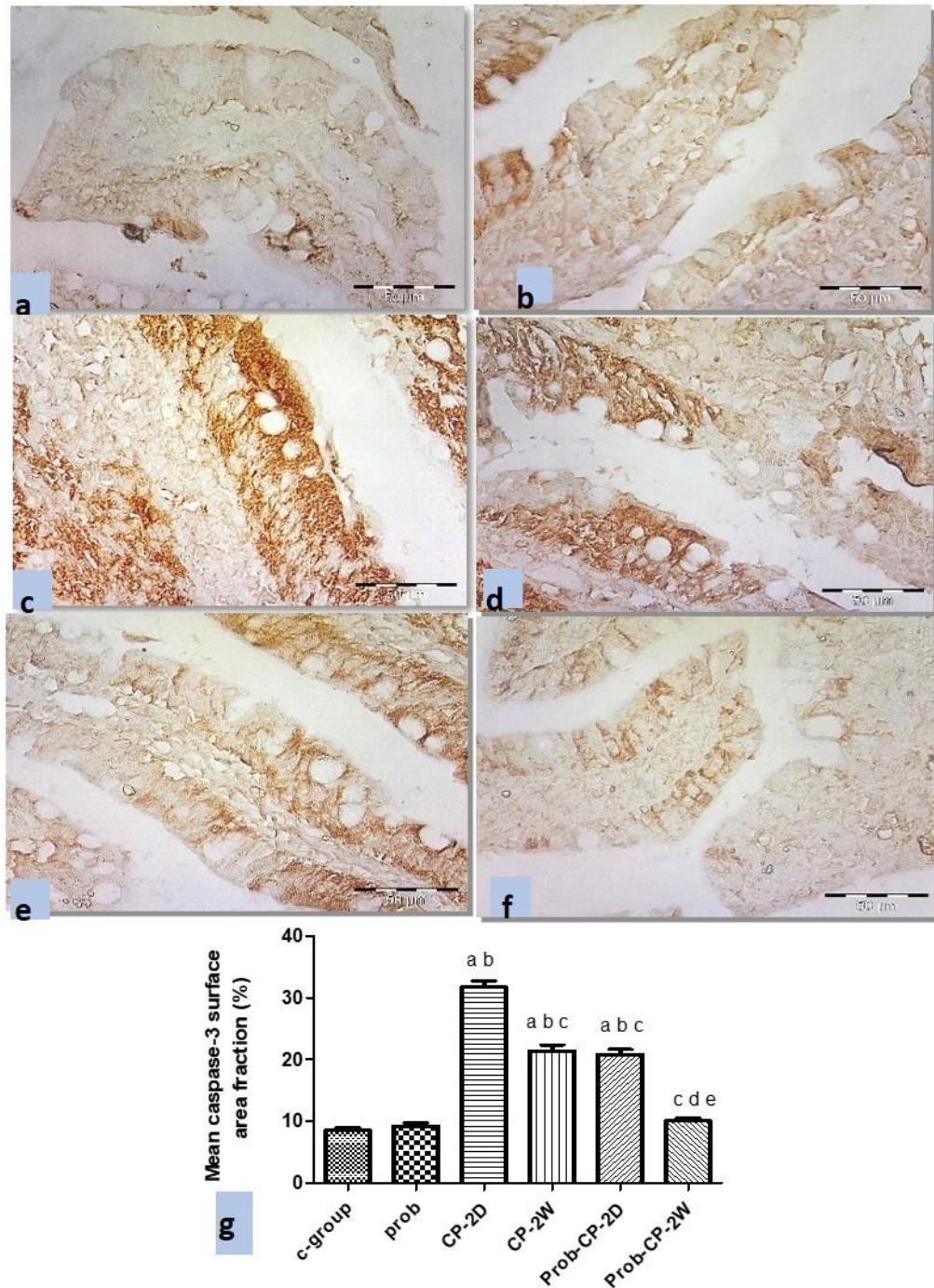


Figure (7): The representative photomicrographs of the jejunum in (a) control and (b) probiotic groups showing immune reactivity for activated caspase-3 scattered in some epithelial cells of the lining of villi (arrows) of jejunal mucosa. (c) CP-2D group showing extensively increased immune positive cells in the lining of villi (arrows). (d) CP-2W and (e) Prob-CP-2D groups showing less immune positive cells in the lining of the villi (arrows). (f) Prob-CP-2W group showing marked decreased immune positive cells in the lining of the villi (arrows). caspase-3 X400. (g) the mean caspase-3 surface area fraction in the studied groups (n=6) a: significant vs C-group, b: significant vs Prob-group, c: significant vs CP-2D, d: significant vs CP-2W, e: significant vs Prob-CP-2D.

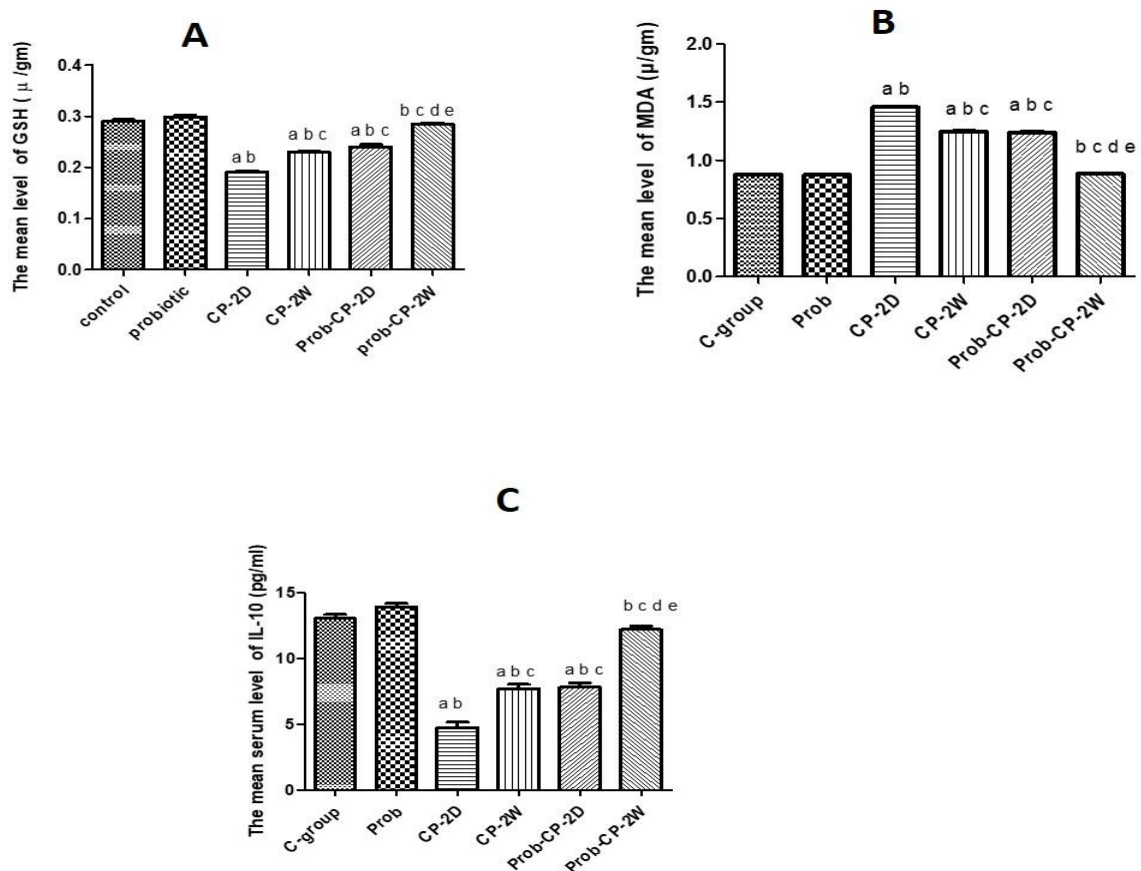


Figure (8): A) The mean level of jejunal MDA (μ/gm) in the studied groups (N=6), B) The mean level of jejunal GSH (μ/gm) in the studied, C) The mean serum level of IL-10 (pg/ml) in the studied groups a: significant vs C-group, b: significant vs Prob-group, c: significant vs CP-2D, d: significant vs CP-2W, e: significant vs Prob-CP-2D

Discussion

Anticancer drugs can damage the intestinal mucosa leading to clinical problems as bacterial translocation, diarrhea, and dyskinesia (Owari et al., 2012). Compared with the duodenum and ileum, the jejunum is the one that has been most severely damaged by chemotherapy (Xie et al., 2016). Cyclophosphamide (CP) is extensively used as an antineoplastic and immunosuppressive agent (Ghobadi et al., 2017). It is cytotoxic, especially to rapidly proliferating cells in the intestinal villi (Shi et al., 2017).

In the current study, 2 days after intraperitoneal injection of CP showed marked morphological changes demonstrating the advanced degree of

tissue injury level. Focal loss of villi and distortion of the remnant villi were in accordance with results of Hamsa and his co-workers (Hamsa and Kuttan, 2010). They owed this to the DNA damage induced by CP through the generation of free radicals or oxidizing species leading to intestinal mucosal injury. They also reported that this mucosal injury impairs gut barrier function and leads to bacterial translocation which results in the systemic inflammatory response. The villous height was significantly decreased while crypt depth was significantly increased in this group. In addition, the V/C ratio was significantly decreased if compared with the C-group. Shortening of the villi and a deepening of the crypts can lead to poor absorption of nutrients

(Shang et al., 2020; Wang et al., 2019). Desquamation of epithelial lining leaving bare areas of mucosa could be explained by Yang and his co-workers (Yang et al., 2013)—who stated that CP suppresses expressions of occludens, zonula occludens 1 (ZO-1), and E-cadherin which play critical role in regulating intestinal mucosa permeability and physical barrier function. The intestinal physical barrier function depends on the integrity of the intercellular junctions, that rely on tight junctions which are formed by integral membrane proteins including claudins and occludins as well as the peripheral membrane proteins including the zonula occludens (ZO-1, ZO-2, and ZO-3) (Wang et al., 2019). Moreover, Signs of degeneration; cellular vacuolation, ballooning, and nuclear pyknosis were founded in the cells lining crypts of jejunum. These vacuolations were similarly founded in liver cells exposed also to CP (AboZaid et al., 2020)

Oxidative stress, which arises as a result of the imbalance between reactive oxygen species (ROS) and the endogenous antioxidant system (Morsy et al., 2020) could explain the congestion and inflammatory cell infiltration of blood vessels in jejunal connective tissue. The CP induced oxidative stress in rats which activated multiple intracellular signaling pathways, leading to the up regulation of pro-inflammatory cytokine production. This was due to the accumulation of inflammatory neutrophils, macrophages, and lymphocytes through the release of proteolytic enzymes and free radicals (Abdel-Hafez et al., 2017b; Hamsa and Kuttan, 2010).

Widely separated muscle fibers (caused by edema) observed in the current study were in accordance with Abd-ElAleem and his co-workers (Abd-ElAleem et al., 2012) who showed that CP caused edema separating the smooth muscle layers of the urinary bladder.

Goblet cells of mucosal surface are part of the first-line protection that help host defense against possible pathogens. They secrete mucins that act as a medium for lubrication and prevent the penetration of the intestinal bacterium in the epithelium barrier (Xie et al., 2016). Indeed, goblet cells could form goblet cell-associated antigen passages and delivered

luminal substances to underlying lamina propria antigen-presenting cells in a manner capable of inducing adaptive immune responses (Knoop and Newberry, 2018).

By using PAS staining, the CP-2D group showed loss of most apical brush borders and basement membranes of the enterocytes of the intestinal villi which might be owed to desquamation of enterocytes. The mean number of goblet cells was significantly decreased within the disturbed epithelial lining. The decreased mucus production in the CP-treated rats probably resulted in the reduction of the intestinal immune function (Ying et al., 2019) and enhanced the risk of pathogens invading the first line of defense of the intestine, and then the related diseases might develop, such as Crohn's disease and inflammatory bowel disease (IBD) (Chen et al., 2019).

The Ki-67 antigen is a proliferation associated nuclear antigen. It is only detected in dividing cells (G1-, S-, G2- and M-phase) and not in quiescent cells (G0 phase) (Li et al., 2015b). It is widely used as a proliferation indicator (Miller et al., 2018). One of the fastest proliferating tissues in the body is the intestinal epithelium. Epithelial cells are constantly being produced within the intestinal crypts and differentiating into specialized absorptive cells as they migrate towards the lumen. Cell proliferation is particularly rapid as the entire lining of the small intestine is replaced every 2 to 3 days in the rodent and 5 to 6 days in humans (Bowen et al., 2006). This was clearly founded in the current study where Ki-67 immune positive cells in both control and probiotic groups were high. There was a significant decrease in the number of Ki-67 positive immunostaining cells in CP-2D group compared to both control and probiotic groups. There are several potential mechanisms by which CP might affect proliferation. The metabolites of CP; phosphoramidate mustard and acrolein, either kill cells immediately or disrupt their functioning, particularly their ability to replicate (Owari et al., 2012). It is supported by previous study which stated that the application of *probiotic* had been proven to decrease the production of reactive oxygen species such as H₂O₂, reducing colonic damage, and inflammation, consequently

projecting on tumor invasion and proliferation (Górska et al., 2019).

Caspases play a key role in apoptosis that could be used as an apoptotic marker (Abdel-Hafez et al., 2017a). In this study, there was a significant increase in the area fraction of caspase-3 positive cells in CP-2D group if compared to both control and probiotic groups. It was supported by Owari and his co-workers (Owari et al., 2012) who stated that CP damage the DNA through the generation of free radicals or oxidizing species. Also, its active metabolite (phosphoramidate mustered) causes DNA cross-linking resulting in cell death either by apoptosis or necrosis (Madondo et al., 2016). These also could be explained by another study (Abdelaziz et al., 2019) that reported that CP induces oxidative damage through decreasing the activities of the antioxidant enzymes and increases the extent of the lipid peroxidation. Oxidative damage is capable of inducing apoptosis, a programmed cell death (Wu et al., 2019a).

The previous histological and histochemical changes occurred in this study were confirmed by its biochemical results. The CP-2D group showed a significant increase in the level of MDA with a significant decrease in GSH level indicating induction of a state of oxidative stress by CP. Increased malondialdehyde (MDA) concentrations in serum appeared to result from an increase of reactive oxygen species as a result of stress in the rats with CP intoxication (Hamsa and Kuttan, 2010). Measurement of MDA activities can serve as an indication of antioxidant because it is a major production of lipid peroxidation and can measure free radical generation (Chen et al., 2019). Furthermore, decreased glutathione (GSH) levels could be explained by direct conjugation of acrolein with GSH, causing GSH depletion. The depletion of GSH decreases the cells' defense against free radical induced injury, and necrotic cell death is the result (Quita and Balbaid, 2015).

Interleukin-10 (IL-10) is a potent anti-inflammatory cytokine and the deficiency can aggravate inflammation in the pathogenesis state (Han et al., 2020). It is produced by many cells of the adaptive immune system, including Th1, Th2 and Th17 cell subsets, regulatory T

cells (Treg cells), cytotoxic T lymphocytes (CD8+ T cells) and B lymphocytes (Fu et al., 2018). In this study, IL-10 levels showed a significant decrease 2 days after CP administration if compared to control and probiotic groups which was in agreement with the results of Han and his co-workers (Han et al., 2020). However, this was in contrast to Wang and his co-workers (Wang et al., 2019) who reported insignificant decrease in serum IL-10 level induced by CP which might be explained by the different dose of CP used in this study.

On the other hand, two weeks after CP administration, jejunal sections showed lower level of injury than in CP-2D group. It was in the form of restoration of more frequent villi, but they appeared shorter and broader with decreased shedding of the epithelium. A significant decrease in crypt depth was observed compared to CP-2D group. Connective tissue showed less congested blood capillaries and inflammatory cells. Awadallah and his co-workers (Awadallah et al., 2020) found a significant reduction in thickness of the main olfactory epithelium of CP mice after two days of CP administration. Then, the main olfactory epithelium was beginning to thicken in CP mice until it was nearly equivalent to saline mice. This agreed with the current results.

PAS sections of CP-2W group showed presence of focal loss of the PAS-stained brush borders and basement membranes of enterocytes. However, goblet cells were significantly increased if compared to CP-2D group but still significantly decreased when compared to C-group.

Cellular proliferation started to increase as there were areas of stratification of polyhedral cells observed in the villi and a significant increase in Ki-67 immune positive cells in the epithelial lining of the crypts 2 weeks after CP administration if compared to CP-2D group. This was explained by Abdel-Hafez and his co-workers (Abdel-Hafez et al., 2017b) who reported that CP treatment killed a fraction of the stem cells, but the loss was well compensated by increased self-renewal that occurs after that cell loss. Once cell proliferation was reinitiated, cell renewal continued at higher

than normal rates for 30 days or more post injection (Awadallah et al., 2020).

Moreover, a significant decrease in the area fraction of caspase-3 immune positive cells was observed in CP-2W group if compared to CP-2D group.

These changes could be explained by the changes in the biochemical results of this study where CP-2W group showed a significant decrease in the MDA level and a significant increase in the GSH level and serum IL-10 level if compared to CP-2D group, but still with a significant difference if compared to the C-group.

Probiotic therapies have been clinically evaluated and used as treatment for human inflammatory bowel disorders and irritable bowel syndrome because of their anti-apoptotic and anti-inflammatory effects (Ciorba et al., 2012). Accumulated data showed that probiotics have beneficial effects on intestinal morphology, microflora population, absorption of nutrients, body antioxidative capacity, and immune response, that consequently improve the gut health (Wu et al., 2019a). Based on their health benefits, probiotics are gaining more attention in biomedical research (Olaniyan and Okotie, 2020).

In the current study administration of probiotics after CP accelerates and enhances the physiological improvement and healing of jejunal mucosa; as 2days of probiotic administration has the same therapeutic effects observed 2weeks after CP withdrawal and 2weeks of probiotic treatment was quite enough to take the histological structure of the jejunal back to its normal architecture.

Administration of probiotics for 2 days after CP injection resulted in the same improvement in the jejunal structure as 2weeks after some sort of withdrawal effects of CP where all the morphological changes were improved but still with a significant difference if compared to the C-group and insignificant if compared to CP-2W group. There was restoration of villi but still appeared shorter and broader with decreased shedding of the epithelium, decreased vascular congestion, inflammatory cell infiltration and edema. These findings had

already been reported as mentioned by Smith and his co-workers (Smith et al., 2008), who observed that *Lactobacillus fermentum* was effective in reducing jejunal inflammation in their model of intestinal mucositis.

Some mechanisms related to the probiotics may contribute to their protective effects, such as the reduction in certain pro-inflammatory cytokines, activation of “natural killer” macrophages and lymphocytes, and stimulation of both immature leukocyte production and interferon production. Probiotics enhance innate immunity and modulate pathogen-induced inflammation, resulting in phagocytosis of the pathogen (Gerhard et al., 2017).

Areas of stratification of polyhedral cells with rounded nuclei and a significant increase in the number of Ki-67 immune positive cells were noticed which proved that probiotics could increase cell proliferation and renewal which appeared early after only two days.

Butyric acid, one of the short chain fatty acids (SCFAs), is an essential energy source for intestinal epithelium that may regulate epithelial cell growth and immune response, provide protection against the intestinal diseases (Hu et al., 2012) and maintain the intestinal epithelial integrity by stimulating epithelial cell proliferation and mucus secretion (Thorburn et al., 2014). Thus, the ameliorative effect of probiotics might be attributed to their ability to increase SCFAs production as mentioned by Li and his co-workers (Li et al., 2015a).

The Prob-CP-2D group preserved brush borders and basement membranes of some areas while other areas remained with lost brush borders of the enterocytes. The number of goblet cells was significantly increased if compared to CP-2D group and insignificantly increased if compared to CP-2W group. This was in accordance with other studies (Forte et al., 2018; Xie et al., 2016) which suggested that the protective effect of lactobacilli on intestinal mucosal integrity may derive from the ability to promote mucins secretion in goblet cells. Probiotics could also cause upregulation of MUC2 (Mucin 2, Oligomeric Mucus/Gel-Forming) gene expression leading

to an increase of 60% of basal luminal mucin contents (Prisciandaro et al., 2011). Cervantes and his co-workers (Cervantes-Barragan et al., 2017) found that probiotics have the ability to induce lamina propria lymphocytes to secrete Interleukin 22(IL-22) which activates intestinal stem cells to regenerate (Hou et al., 2018). Thus, probiotics could improve the intestinal cell proliferation (Marsova et al., 2020). In the current study, the number of Ki-67 immune positive cells of the intestinal glands was significantly increased in this group if compared to Cp-2D group without significant difference if compared to CP-2W group. It could be also explained as the probiotics could increase the number of paneth cells. Paneth cells could modulate the proliferation and differentiation of intestinal stem cells according to this research study (Mei et al., 2020).

Apoptotic cells were significantly decreased in Prob-Cp-2D group when compared to CP-2D group without significant difference if compared to CP-2W group. This was in accordance with Li and his co-workers (Li et al., 2015a). This could be explained as probiotics have antiapoptotic effect on both small and large intestine by increasing SCFAs production (Wu et al., 2019b).

Moreover, administration of probiotics for 2 days after CP injection showed a significant decrease in the MDA level and a significant increase in the GSH level if compared to CP-2D group without significant difference if compared to CP-2W group. Probiotics could decrease MDA levels and increase GSH levels due to its ability to release the antioxidant dipeptide, Gamma-L-Glutamyl-L-cysteine (γ -Glu-Cys) which is the most immediate precursor to the antioxidant glutathione (Mishra et al., 2015). Administration of probiotics in the study of Byun and his co-workers (Byun et al., 2016) improved survival rates of small intestinal injuries. They added that improvements appeared to be associated with decrease in pro-inflammatory cytokines such as IL-6 and TNF- α , and an increase of IL-10, an anti-inflammatory cytokine which agreed with our results. The increased expression of anti-inflammatory IL-10 induced by some probiotic strains can be beneficial to the host (De Montijo-Prieto et al., 2015).

Taken together, probiotics administration for 2 days could shorten the time of healing from 2 weeks in CP-2W group to 2 days in Prob-CP-2D group. Moreover, administration of probiotics for 2 weeks after CP injection in this study resulted in marked amelioration of the damaging effects of CP. The morphological changes improved showing insignificant difference compared to C-group. Prob-CP-2W group-stained sections showed more frequent villi that appeared more or less normal and retained their covering; simple columnar epithelium and goblet cells. The crypt depth was significantly decreased, and the villous height and V/C ratio was elevated. No obvious vascular congestion or inflammatory cell infiltration. These results were in agreement with results of Kumar and his co-workers (Kumar et al., 2015) who found similar effects of *Lactobacillus plantarum* 21 in ulcerative colitis.

Also, most of PAS brush borders of the columnar cells and basement membranes of the villi and crypts were preserved. We noticed a significant increase in the number of the goblet cells which were nearly similar to those of C-group with insignificant difference. In addition, probiotics could restore proliferation and suppress apoptosis in intestinal mucosa (Wu et al., 2019b). This was evidenced in the Prob-CP-2W group that showed a significant increase in the number of Ki-67 immune positive cells a significant decrease in the apoptotic cells to levels which were insignificant if compared to C-group.

The laboratory findings showed that administration of probiotics for 2 weeks after CP injection showed a significant decrease in MDA level and a significant increase in GSH level and serum Il-10 level if compared to CP-2D, CP-2W and Prob-CP-2D groups becoming nearly similar to those of C-group with insignificant difference. These results were in accordance with Kumar and his co-workers (Kumar et al., 2015) who stated that *Lactobacillus plantarum* 21 relieved the condition of oxidative stress in trinitrobenzenesulfonic acid (TNBS)-induced ulcerative colitis in rats.

Thus, two weeks of probiotics administration augmented their effects and restored more or

less normal intestinal tissues counteracting the effects of CP by the same mechanisms mentioned previously.

Taken together it could be concluded that CP induced a condition of oxidative stress and inflammation leading to jejunal morphological changes including mucosal barrier damage, cellular apoptosis, and inhibition of epithelial regeneration. While administration of probiotics gradually ameliorated these effects through their anti-oxidative, anti-inflammatory, anti-apoptotic effects and through stimulation of epithelial cell proliferation and hence regeneration.

Funding

This research did not receive any specific grant from funding agencies in the public, commercial, or not-for-profit sectors.

Declaration of interest

There is no conflict of interest.

Availability of data and materials

The data that support the findings of this study are available from the corresponding author upon reasonable request.

References

1. Abd-ElAleem, S.A., Ahmed, H.M., El-Tahawy, N.F., Abdalla, A.M., Kamel, B.A.J.M.J.o.F.M., and Toxicology, C. (2012). Protective Role of Nigella Sativa Oil in Chronic Cyclophosphamide Toxicity on Urinary Bladder and Liver's Rats. *20*, 29-56.
2. Abdel-Hafez, S., Rifaai, R., and Abd, W.E. (2017a). Mechanism of grape seeds extract protection against paracetamol renal cortical damage in male Albino rats. *Bratislavske lekarske listy 118*, 233-242.
3. Abdel-Hafez, S.M.N., Rifaai, R.A., and Abdelzaher, W.Y. (2017b). Possible protective effect of royal jelly against cyclophosphamide induced prostatic damage in male albino rats; a biochemical, histological and immuno-histochemical study. *Biomed Pharma-cother 90*, 15-23.
4. Abdelaziz, T.E., Borai, E.-B.N., Kamal, K.H., Hanem, E.-G.J.G.B., and Sciences, P. (2019). Contribution of garlic for improving the cytoprotective effect of mesna against cyclophosphamide toxicity in rats. *7*, 008-020.
5. AboZaid, S., Abobakr, A., Hasssan, A., and Malak, M.J.J.o.M.R. (2020). The possible protective effect of captopril on liver and bone marrow after cyclophosphamide-induced toxicity in adult albino rats.
6. Ahlmann, M., and Hempel, G. (2016). The effect of cyclophosphamide on the immune system: implications for clinical cancer therapy. *Cancer Chemother Pharmacol 78*, 661-671.
7. Alhowail, A., Sajid, S., Almogbel, Y., Rabbani, S., and Alsharidah, M.J.J.o.P.R.I. (2019). Effect of Cyclophosphamide and Its Combination with Metformin on the Survival Rate in Mice. 1-6.
8. Awadallah, N., Proctor, K., Joseph, K.B., Delay, E.R., and Delay, R.J.J.C.S. (2020). Cyclophosphamide has Long-Term Effects on Proliferation in Olfactory Epithelia. *45*, 97-109.
9. Bowen, J.M., Gibson, R.J., Cummins, A.G., and Keefe, D.M. (2006). Intestinal mucositis: the role of the Bcl-2 family, p53 and caspases in chemotherapy-induced damage. *Support Care Cancer 14*, 713-731.
10. Byun, S.J., Lim, T.J., Lim, Y.J., Seo, J.G., and Chung, M.J. (2016). In vivo effects of s-pantoprazole, polaprenzinc, and probiotic blend on chronic small intestinal injury induced by indomethacin. *Benef Microbes 7*, 731-737.
11. Cervantes-Barragan, L., Chai, J.N., Tianero, M.D., Di Luccia, B., Ahern, P.P., Merriman, J., Cortez, V.S., Caparon, M.G., Donia, M.S., and Gilfillan, S.J.S. (2017). Lactobacillus reuteri induces gut intraepithelial CD4+ CD8αα+ T cells. *357*, 806-810.
12. Chen, S., Wang, J., Fang, Q., Dong, N., and Nie, S.J.F.H. (2019). Polysaccharide from natural Cordyceps sinensis ameliorated intestinal injury and enhanced antioxidant activity in immunosuppressed mice. *89*, 661-667.
13. Ciorba, M.A., Riehl, T.E., Rao, M.S., Moon, C., Ee, X., Nava, G.M., Walker, M.R., Marinshaw, J.M., Stappenbeck, T.S., and Stenson, W.F. (2012). Lactobacillus probiotic protects intestinal epithelium from radiation injury in a TLR-2/cyclo-oxygenase-2-dependent manner. *Gut 61*, 829-838.

14. de LeBlanc, A.d.M., and LeBlanc, J.G.J.W.J.o.G.W. (2014). Effect of probiotic administration on the intestinal microbiota, current knowledge and potential applications. *20*, 16518.
15. De Montijo-Prieto, S., Moreno, E., Bergillos-Meca, T., Lasserrot, A., Ruiz-Lopez, M.D., Ruiz-Bravo, A., and Jimenez-Valera, M. (2015). A *Lactobacillus plantarum* strain isolated from kefir protects against intestinal infection with *Yersinia enterocolitica* O9 and modulates immunity in mice. *Res Microbiol 166*, 626-632.
16. Farkas, P., Könczöl, F., Lőrinczy, D.J.J.o.T.A., and Calorimetry (2019). Monitoring the side effects with DSC caused by cyclophosphamide treatment. 1-6.
17. Forte, C., Manuali, E., Abbate, Y., Papa, P., Vieceli, L., Tentellini, M., Trabalza-Marinucci, M., and Moscati, L. (2018). Dietary *Lactobacillus acidophilus* positively influences growth performance, gut morphology, and gut microbiology in rurally reared chickens. *Poult Sci 97*, 930-936.
18. Fu, Y.P., Feng, B., Zhu, Z.K., Feng, X., Chen, S.F., Li, L.X., Yin, Z.Q., Huang, C., Chen, X.F., Zhang, B.Z., *et al.* (2018). The Polysaccharides from *Codonopsis pilosula* Modulates the Immunity and Intestinal Microbiota of Cyclophosphamide-Treated Immunosuppressed Mice. *Molecules 23*, 1801.
19. Garcia-Oliveira, P., Otero, P., Pereira, A.G., Chamorro, F., Carpena, M., Echave, J., Fraga-Corral, M., Simal-Gandara, J., and Prieto, M.A. (2021). Status and Challenges of Plant-Anticancer Compounds in Cancer Treatment. *Pharmaceuticals 14*, 157.
20. Gerhard, D., Sousa, F., Andraus, R.A.C., Pardo, P.E., Nai, G.A., Neto, H.B., Messoria, M.R., and Maia, L.P. (2017). Probiotic therapy reduces inflammation and improves intestinal morphology in rats with induced oral mucositis. *Braz Oral Res 31*, e71.
21. Ghobadi, E., Moloudizargari, M., Asghari, M.H., and Abdollahi, M. (2017). The mechanisms of cyclophosphamide-induced testicular toxicity and the protective agents. *Expert Opin Drug Metab Toxicol 13*, 525-536.
22. Górska, A., Przystupski, D., Niemczura, M.J., and Kulbacka, J. (2019). Probiotic bacteria: a promising tool in cancer prevention and therapy. *Current microbiology 76*, 939-949.
23. Hamsa, T.P., and Kuttan, G. (2010). *Ipomoea obscura* ameliorates cyclophosphamide-induced toxicity by modulating the immune system and levels of proinflammatory cytokine and GSH. *Can J Physiol Pharmacol 88*, 1042-1053.
24. Han, X., Bai, B., Zhou, Q., Niu, J., Yuan, J., Zhang, H., Jia, J., Zhao, W., and Chen, H. (2020). Dietary supplementation with polysaccharides from *Ziziphus Jujuba* cv. *Pozao* intervenes in immune response via regulating peripheral immunity and intestinal barrier function in cyclophosphamide-induced mice. *Food Funct 11*, 5992-6006.
25. Hassan, I., Ebaid, H., Alhazza, I.M., Al-Tamimi, J., Aman, S., and Abdel-Mageed, A.M. (2019). Copper Mediates Anti-Inflammatory and Antifibrotic Activity of Gleevec in Hepatocellular Carcinoma-Induced Male Rats. *Can J Gastroenterol Hepatol 2019*, 9897315.
26. Hou, Q., Ye, L., Liu, H., Huang, L., Yang, Q., Turner, J., Yu, Q.J.C.D., and Differentiation (2018). *Lactobacillus* accelerates ISCs regeneration to protect the integrity of intestinal mucosa through activation of STAT3 signaling pathway induced by LPLs secretion of IL-22. *25*, 1657-1670.
27. Hu, J.L., Nie, S.P., Min, F.F., and Xie, M.Y. (2012). Polysaccharide from seeds of *Plantago asiatica* L. increases short-chain fatty acid production and fecal moisture along with lowering pH in mouse colon. *J Agric Food Chem 60*, 11525-11532.
28. Knoop, K.A., and Newberry, R.D.J.M.i. (2018). Goblet cells: multifaceted players in immunity at mucosal surfaces. *11*, 1551-1557.
29. Kumar, C.S., Reddy, K.K., Reddy, A.G., Vinoth, A., CH, S.R.C., Boobalan, G., and Rao, G.J.I.i. (2015). Protective effect of *Lactobacillus plantarum* 21, a probiotic on trinitrobenzenesulfonic acid-induced ulcerative colitis in rats. *25*, 504-510.

30. Li, C., Nie, S.P., Zhu, K.X., Xiong, T., Li, C., Gong, J., and Xie, M.Y. (2015a). Effect of *Lactobacillus plantarum* NCU116 on loperamide-induced constipation in mice. *Int J Food Sci Nutr* 66, 533-538.
31. Li, L.T., Jiang, G., Chen, Q., and Zheng, J.N.J.M.m.r. (2015b). Ki67 is a promising molecular target in the diagnosis of cancer. *11*, 1566-1572.
32. Madondo, M.T., Quinn, M., and Plebanski, M. (2016). Low dose cyclophosphamide: Mechanisms of T cell modulation. *Cancer Treat Rev* 42, 3-9.
33. Marsova, M., Odorskaya, M., Novichkova, M., Polyakova, V., Abilev, S., Kalinina, E., Shtil, A., Poluektova, E., and Danilenko, V. (2020). The *Lactobacillus brevis* 47 f Strain Protects the Murine Intestine from Enteropathy Induced by 5-Fluorouracil. *Microorganisms* 8, 876.
34. Mei, X., Gu, M., and Li, M. (2020). Plasticity of Paneth cells and their ability to regulate intestinal stem cells. *Stem Cell Res Ther* 11, 349.
35. Miller, I., Min, M., Yang, C., Tian, C., Gookin, S., Carter, D., and Spencer, S.L.J.C.r. (2018). Ki67 is a graded rather than a binary marker of proliferation versus quiescence. *24*, 1105-1112. e1105.
36. Mishra, V., Shah, C., Mokashe, N., Chavan, R., Yadav, H., Prajapati, J.J.J.o.a., and chemistry, F. (2015). Probiotics as potential antioxidants: a systematic review. *63*, 3615-3626.
37. Moron, M.S., Depierre, J.W., and Mannervik, B. (1979). Levels of glutathione, glutathione reductase and glutathione S-transferase activities in rat lung and liver. *Biochim Biophys Acta* 582, 67-78.
38. Morsy, M.A., Abdel-Aziz, A.M., Abdel-Hafez, S., Venugopala, K.N., Nair, A.B., and Abdel-Gaber, S.A. (2020). The Possible Contribution of P-Glycoprotein in the Protective Effect of Paeonol against Methotrexate-Induced Testicular Injury in Rats. *Pharmaceuticals* 13, 223.
39. Olaniyan, O., and Okotie, G. (2020). Nutritional Physiology. In *Innovations in Food Technology* (Springer), pp. 395-424.
40. Owari, M., Wasa, M., Oue, T., Nose, S., and Fukuzawa, M. (2012). Glutamine prevents intestinal mucosal injury induced by cyclophosphamide in rats. *Pediatr Surg Int* 28, 299-303.
41. Prisciandaro, L.D., Geier, M.S., Butler, R.N., Cummins, A.G., and Howarth, G.S. (2011). Probiotic factors partially improve parameters of 5-fluorouracil-induced intestinal mucositis in rats. *Cancer Biol Ther* 11, 671-677.
42. Quita, S.M., and Balbaid, S.O.J.E.p. (2015). The protective effect of lemon fruit extract on histopathological changes induced in small intestines and pancreas of male mice by cyclophosphamide. *7*, 1412.
43. Satish Kumar, C.S., Kondal Reddy, K., Reddy, A.G., Vinoth, A., Ch, S.R., Boobalan, G., and Rao, G.S. (2015). Protective effect of *Lactobacillus plantarum* 21, a probiotic on trinitrobenzenesulfonic acid-induced ulcerative colitis in rats. *Int Immunopharmacol* 25, 504-510.
44. Shang, X., He, X., Liu, H., Wen, B., Tan, T., Xu, C., Niu, W., and Zhang, Y.J.S.S. (2020). Stachyose Prevents Intestinal Mucosal Injury in the Immunosuppressed Mice. *72*, 1900073.
45. Shi, H., Chang, Y., Gao, Y., Wang, X., Chen, X., Wang, Y., Xue, C., and Tang, Q. (2017). Dietary fucoidan of *Acaudina molpadioides* alters gut microbiota and mitigates intestinal mucosal injury induced by cyclophosphamide. *Food Funct* 8, 3383-3393.
46. Smith, C.L., Geier, M.S., Yazbeck, R., Torres, D.M., Butler, R.N., and Howarth, G.S. (2008). *Lactobacillus fermentum* BR11 and fructo-oligosaccharide partially reduce jejunal inflammation in a model of intestinal mucositis in rats. *Nutr Cancer* 60, 757-767.
47. Suvarna, K.S., Layton, C., and Bancroft, J.D. (2018). *Bancroft's Theory and Practice of Histological Techniques E-Book* (Elsevier Health Sciences).
48. Thorburn, A.N., Macia, L., and Mackay, C.R.J.I. (2014). Diet, metabolites, and "western-lifestyle" inflammatory diseases. *40*, 833-842.
49. Uchiyama, M., and Mihara, M.J.A.b. (1978). Determination of malonaldehyde precursor in tissues by thiobarbituric acid test. *86*, 271-278.

50. Wang, X., Yuan, Z., Zhu, L., Yi, X., Ou, Z., Li, R., Tan, Z., Pozniak, B., Obminska-Mrukowicz, B., Wu, J., *et al.* (2019). Protective effects of betulinic acid on intestinal mucosal injury induced by cyclophosphamide in mice. *Pharmacol Rep* 71, 929-939.
51. Wu, Y., Wang, B., Zeng, Z., Liu, R., Tang, L., Gong, L., and Li, W. (2019a). Effects of probiotics *Lactobacillus plantarum* 16 and *Paenibacillus polymyxa* 10 on intestinal barrier function, antioxidative capacity, apoptosis, immune response, and biochemical parameters in broilers. *Poult Sci* 98, 5028-5039.
52. Wu, Y., Wang, B., Zeng, Z., Liu, R., Tang, L., Gong, L., and Li, W.J.P.s. (2019b). Effects of probiotics *Lactobacillus plantarum* 16 and *Paenibacillus polymyxa* 10 on intestinal barrier function, antioxidative capacity, apoptosis, immune response, and biochemical parameters in broilers. 98, 5028-5039.
53. Xie, J., Nie, S., Yu, Q., Yin, J., Xiong, T., Gong, D., and Xie, M. (2016). *Lactobacillus plantarum* NCU116 Attenuates Cyclophosphamide-Induced Immunosuppression and Regulates Th17/Treg Cell Immune Responses in Mice. *J Agric Food Chem* 64, 1291-1297.
54. Yang, J., Liu, K.X., Qu, J.M., and Wang, X.D. (2013). The changes induced by cyclophosphamide in intestinal barrier and microflora in mice. *Eur J Pharmacol* 714, 120-124.
55. Ying, M., Yu, Q., Zheng, B., Wang, H., Wang, J., Chen, S., Gu, Y., Nie, S., and Xie, M.J.J.o.F.F. (2019). Cultured *Cordyceps sinensis* polysaccharides attenuate cyclophosphamide-induced intestinal barrier injury in mice. 62, 103523.
56. Ying, M., Yu, Q., Zheng, B., Wang, H., Wang, J., Chen, S., Nie, S., and Xie, M. (2020). Cultured *Cordyceps sinensis* polysaccharides modulate intestinal mucosal immunity and gut microbiota in cyclophosphamide-treated mice. *Carbohydr Polym* 235, 115957.